Linear dunes on Titan and earth: Initial remote sensing comparisons

J. Radebaugh [a,*], R. Lorenz [b], T. Farr [c], P. Paillou [d], C. Savage [a], C. Spencer [a]

[a] Department of Geological Sciences, Brigham Young University, Provo, UT 84602, United States
[b] Space Department, Johns Hopkins University Applied Physics Lab, Laurel, MD 20723, United States
[c] Jet Propulsion Laboratory, California Institute of Technology, 4800 Oak Grove Drive, Pasadena, CA 91109-8099, United States
[d] Observatoire Aquitain des Sciences de l'Univers, UMR 5804, Floirac, France

ARTICLE INFO

ABSTRACT

Thousands of dunes found in Cassini Radar images of the equatorial regions of Titan, a moon around Saturn, are similar in size and morphology to linear dunes on Earth. We present remote sensing images of terrestrial analogues to the dunes on Titan obtained by Landsat and radar, both at considerably higher resolution than are available at Titan, that provide information about dune landforms and processes. Dunes are generally dark to radar, indicating smooth surfaces and signal absorbing materials, but at certain incidence angles, dune surfaces can reflect the radar signal and lead to a bright return. Linear dunes on Titan and Earth diverge around topographic obstacles, creating teardrop patterns that indicate mean direction of wind flow and sand transport. When sand supply or wind conditions change in linear dune fields, such as behind an obstacle or near the margin of the dune field, dunes disappear, change size and spacing, or change dune type. These comparisons of features on Titan and Earth provide a better understanding of the global, sand-transporting wind directions, sand properties and supply, and the nature of the underlying substrate, on Titan.

© 2009 Elsevier B.V. All rights reserved.

1. Introduction

Vast fields of dunes have been discovered on Titan, the largest moon around Saturn (Lorenz et al., 2006), a world that is at once very different from Earth, yet also similar in many ways (e.g. Lorenz and Mitton, 2008). Titan is a cold, icy world, with a surface gravity similar to the Moon around Earth. It is somewhat larger (5150 km diameter) than the planet Mercury and, uniquely among the moons of the solar system, has a thick atmosphere (1.5 bar surface pressure) predominantly of nitrogen with some methane. The action of sunlight on this methane produces heavier organic compounds, some of which accumulate as solids on the surface, and are sculpted by winds into dunes. Thousands of linear duneforms have been observed by the Cassini Radar instrument on the Cassini spacecraft, operating in Synthetic Aperture Radar (SAR) mode. These features are found mainly in equatorial regions, dominantly within ± 30° of the equator, and they nearly encircle the globe. They may cover as much as 20% of the surface and have orientations indicative of time-averaged, W to E wind flow across the globe (Lorenz et al., 2006; Radebaugh et al., 2008).

Dunes have also been observed by other Cassini instruments, the Visual and Infrared Mapping Spectrometer (VIMS), Imaging Science Subsystems (ISS) and the Huygens probe Descent Imager and Spectral Radiometer (DISR) (Tomasko et al., 2005; Barnes et al., 2008). VIMS and ISS observe Titan during Cassini flybys of Titan (every few weeks

since 2004, and presently planned to continue through 2010) at near-infrared wavelengths (1–5 μm, and 0.94 μm, respectively) where the atmospheric haze that obscures the surface at visible wavelengths is comparatively transparent. The DISR instrument observed a small part of the surface at visible wavelengths from beneath most of the haze during the Huygens parachute descent in 2005 at 192° W, 10° S. We emphasize in this paper observations by the Cassini Radar instrument, which was optimized for the coverage and resolution necessary to observe large regions of dunes on Titan, although we note that studies of dunes have benefited by analysis of data from all instruments observing dunes. For example, the dunes on Titan are generally dark to Cassini Radar, indicating the dunes have a smooth surface and/or the materials are absorbing at the Cassini Radar wavelength of 2.17 cm (Fig. 1; Lorenz et al., 2006; Radebaugh et al., 2008). The dunes are also dark, however, to VIMS and ISS, operating in the visible and near-infrared region of the spectrum, indicating the dunes are composed mainly of visually dark materials, such as the organics predicted to have precipitated out of the atmosphere (Soderblom et al., 2007; Barnes et al., 2008). In addition, although sand-free interdune areas are visible with Cassini Radar, which may penetrate up to some meters depth through some materials, sand-free interdunes are also visible with VIMS, which only senses the top few micrometers. This has been given as evidence that the dunes are likely active or were so in the recent past, because the high, closely spaced dunes characteristic of linear dune fields have not eroded by mass wasting or fluvial action into the low, interdune areas (Barnes et al., 2008).

Though dune studies on Titan indicate it is useful to utilize several different remote sensing data sets to understand the formation and

---

* Corresponding author. Tel.: +1 801 422 9127; fax: +1 801 422 0267.
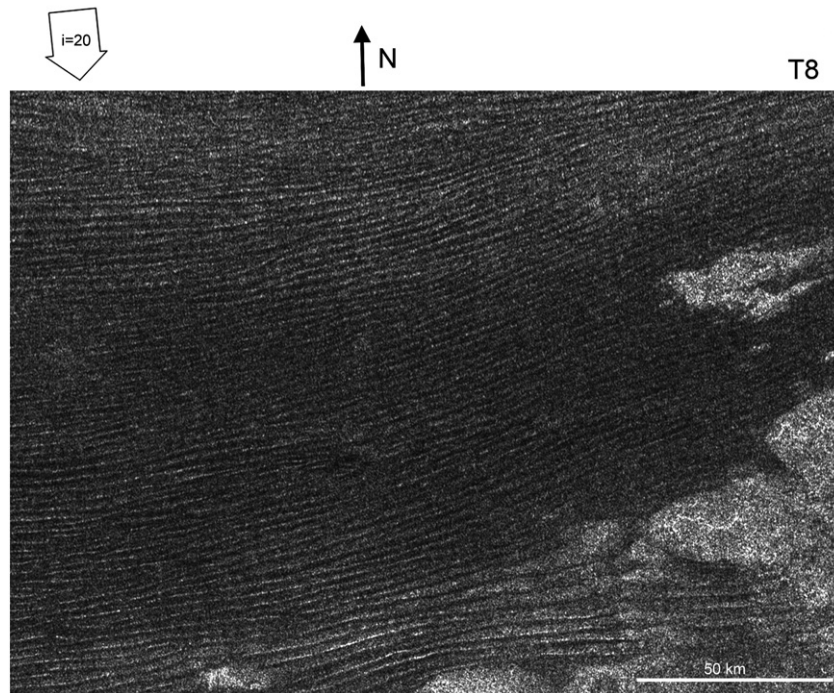E-mail address: jani.radebaugh@byu.edu (J. Radebaugh).

Fig. 1. Equatorial sand sea on Titan imaged by Cassini Radar. Dark linear features are the sides of dunes facing away from the radar, while bright linear features are bright because of direct reflection off a radar-facing slope. Other, non-linear bright features, especially in lower right, are underlying substrate or slightly elevated topographic features. Image obtained during T8 flyby, Oct. 2005, 8° S, 264° W, ~300 m resolution. Hollow arrow indicates incidence angle and direction in all Titan images.

evolution of landforms, it is also beneficial to study better-known or more accessible analogues to improve understanding of features. Terrestrial analogue studies for planetary landforms have been done with great success for many different features (e.g., Campbell and Campbell, 1992; Greeley et al., 1998; Farr, 2004; Zimbelman and Williams, 2007; Keszthelyi and McEwen, 2007). The underlying assumptions behind these studies are that although materials, time scales, and some other fundamental properties, such as gravitational acceleration, may vary across bodies, processes and resultant outcomes, such as landforms, remain inherently similar. Thus, although a "river" on Titan may be carved by liquid methane rainfall onto a water ice surface in a 1.5 bar atmosphere on a 0.14 g surface, the physics that govern the flow of liquids and erosion of bedrock are consistent, scalable, and predictable. We apply this logic to our studies of dunes on Titan by analyzing analogues to the dunes on Titan in sand seas located in many regions across Earth.

This paper highlights the utility of radar images for studies of dune morphology and to compare what is shown in radar and near-infrared images of terrestrial dunes with Cassini Radar images of dunes on Titan. We note that whereas the application of radar data to aeolian studies has been pointed out before (e.g. Blom and Elachi, 1981, 1987; Greeley et al., 1997) relatively few morphological studies of terrestrial dunes have been published using imaging radar data, either examining SAR images directly, e.g. Blumberg (1998) and Qong (2000) or derived topography datasets, e.g. Blumberg (2005). Motivated by the dunes of Titan being most effectively surveyed with Cassini Radar data (although resolvable in other data such as VIMS, those datasets cover a much smaller area at the high resolution necessary to observe individual dunes), we consider what can be learned about morphologies of dunes on Titan through a reexamination of radar and near-infrared images of morphologies of dunes on Earth.

2. Radar vs. V-NIR

Cassini Radar images of Titan are obtained at Ku-band (2.17 cm, 13.78 GHz), operating as the spacecraft flies past Titan at ~1500 km altitude. A swath 120–450 km wide and several thousand kilometers long is created from 5 antenna beams (Elachi et al., 2005). Image resolution varies from 300 m to 1 km, depending on spacecraft range and orbital geometry (spacecraft to surface range ~950 km–5000 km). To date, at the end of the Cassini Prime Mission, 20 Titan SAR image swaths have been obtained over a range of latitudes and longitudes (dominantly equatorial and north polar, leading hemisphere), covering nearly 30% of the surface. The Cassini Radar returns a high signal, translated into high image brightness, for features that are rough, fractured, or facing directly towards the instrument, and a low signal or low image brightness for features that are signal absorbing or smooth (Fig. 2; the incidence angle range of the Cassini Radar is ~15°–40°). Some features can also appear quite different when viewed from different geometries (e.g., Blom and Elachi, 1981, 1987; Blumberg, 1998). Initial studies of dunes on Titan, seen at orthogonal viewing angles, revealed the dunes and substrate differ almost strictly in presence or absence of radar-illuminated dune faces (Radebaugh et al., 2008). The effects of radar illumination from different incidence angles on the dunes have not been systematically studied; however, a more mathematical approach to various aspects of radar illumination effects on dunes on Titan (in the style of Qong, 2000) is underway (LeGall et al., 2008). In addition, the dielectric constant of the material influences the backscattered power: a high dielectric constant leads to a high reflection coefficient and then a stronger radar return.

The two main terrestrial remote sensing data types that we use to compare with Cassini Radar images are radar, a natural choice because of the similarity in wavelength range, and V-NIR, because of the large available dataset and interpretability of the images. On Earth, an extensive radar data set exists from SIR-C/X-SAR (Spaceborne Imaging Radar-C/X-Band Synthetic Aperture Radar; Stofan et al., 1995; Evans et al., 1997), SRTM (Shuttle Radar Topography Mission; Farr et al., 2007) and other orbital and airborne radars. Also many V-NIR satellite images of Earth have been taken from Landsat Thematic Mapper (TM) and Enhanced Thematic Mapper (ETM), ASTER, AVHRR, MODIS, IKONOS, SPOT, IRS and others. Our studies focus on X-SAR, SRTM, and Landsat 7 ETM+, because of the availability, coverage, quality, and resolution, which are better than that of the Cassini Radar images,
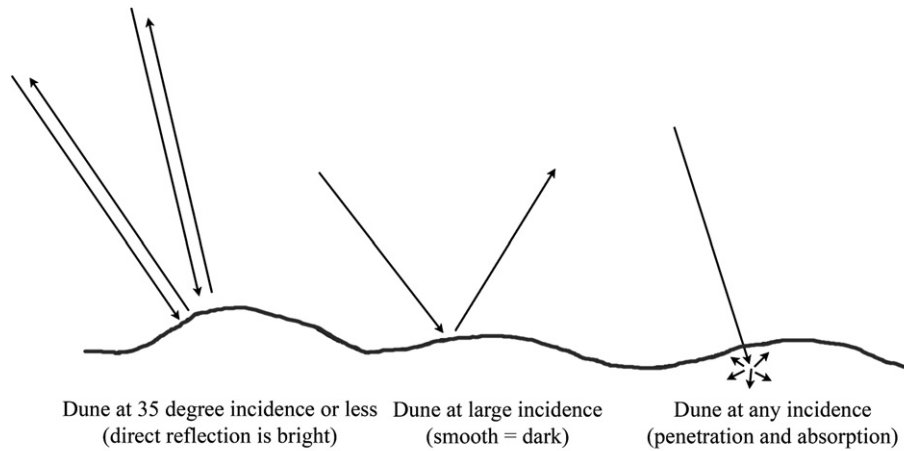
Dune at 35 degree incidence or less   Dune at large incidence   Dune at any incidence
(direct reflection is bright)   (smooth = dark)   (penetration and absorption)

Fig. 2. Incidence angle effects on radar images of dunes. Note that the maximum slope angle of sand on Earth is about 35°, the slip face. Thus, radar signals sent out at this angle or less can be reflected directly back to the radar, causing a strong return.

often by a factor of 10. Most Cassini Radar images are ~300 m resolution, and can be over 1 km. (All Cassini Radar images shown in this paper have resolution ~300 m.) X-SAR images range from 10 m–200 m resolution, typically 30 m, at 3 cm (X-band). The SRTM images used in this study are C-band (5.5 cm), are an average of several passes at varying incidence angles in HH and VV polarizations, and have a resolution of ~30 m. They were also orthorectified using the digital topographic data obtained by SRTM. Areas for which the topographic data could not be processed, however, were left void and are shown as black in the SRTM image data. Landsat 7 ETM+ has a resolution of 30 m for bands 1–5 (~0.5 μm intervals from 0.45–1.75 μm) and 7 (2.1–2.4 μm); a combination of bands 7, 4, and 2 was used to generate the color images in this paper (Markham et al., 2003; NASA online Landsat Handbook, 2008).

Radar and V-NIR image data sets contain different and complementary types of information about the features. In general, radar is used to determine morphological and physical properties of dunes and surroundings, and V-NIR is used to determine morphological and compositional properties. For example, Fig. 3 shows a region in Egypt with extensive linear dunes. The Landsat image, at left, shows clearly the dunes, some sand-free substrate, and details on the dune surfaces, such as small, superimposed dunes and sharp-crested seifs, or dune summits. The X-SAR image on the right differentiates more clearly between the smooth and radar-absorbing sands on the dunes and the sand-free substrate.

2.1. Topography from radar

For V-NIR and radar data sets, be aware of image illumination direction and incidence angle, because these qualities affect the presentation of the surface to the viewer. For V-NIR images, knowledge of illumination direction and incidence angle can help determine slopes and heights of features from shadow measurements, a type of analysis known as photoclinometry (e.g., Davis and Soderblom, 1984; McEwen, 1991). Radar image interpretation is also dependent on radar illumination direction and incidence angle, as the degree of absorption or reflection of a signal by materials depends on these properties (Blom and Elachi, 1987, 1981).

Dunes on Earth often appear radar dark because they have particle sizes that efficiently absorb the radar signal, precluding reflections that can be received at the instrument. The dune surfaces, including ripples and other imperfections, however, could lead to increased scatter. If some of these features are smaller than the radar wavelengths, or if penetration of the signal into the dunes minimizes the effects, a low signal return could occur. On Titan, saltation lengths were calculated to be <1 cm (Lorenz et al., 1995). If, as is debated by eolian scientists, a correlation exists between this length and ripple sizes, the ripples would not be visible by Cassini Radar.

Some dune surfaces may be bright to radar because they present a face directly towards the instrument. This creates a direct bounce effect, leading to a high signal (Figs. 1 and 2; e.g., Blumberg, 1998).
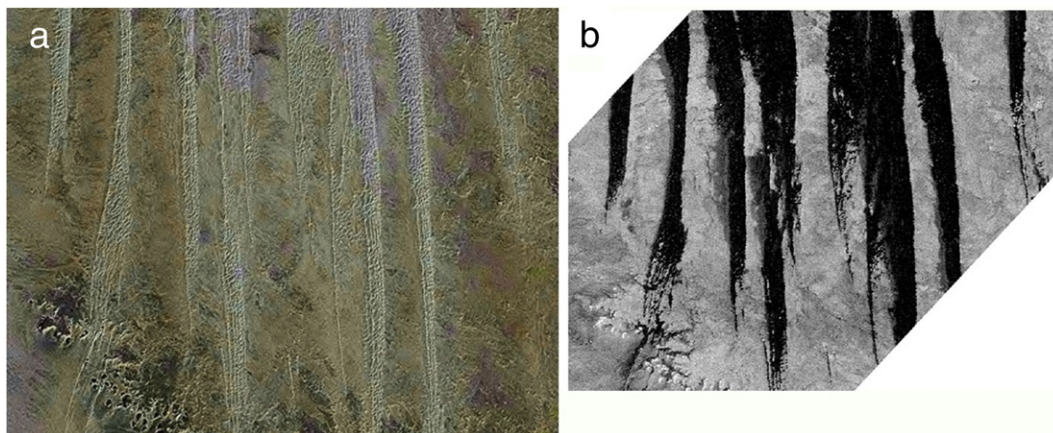

Fig. 3. Linear dune forms in SW Egypt are shown in (a). V-NIR (Landsat) and (b) X-SAR radar images. Underlying bedrock can be seen in both images, but has a higher contrast in the radar image (b), because dune sands are smooth or absorbing to the radar signal whereas the interdune area is rough. Smaller-scale features on the dune summits are illuminated by sunlight from the lower right in the Landsat (a) and by the radar signal (b) from the lower right. Images 32 km across, centered at 26.2° N, 26.9° E. North is up.

Similar to illumination and shadowing in V-NIR images, this information can be used in radar images to determine slopes and heights of features, using a method called radarclinometry (Fig. 2; e.g. Kirk et al., 2005; Radebaugh et al., 2007). This method has been used for some regions on Titan that display slope reflections, such as in the Belet sand sea, near 8° S, 265° W (Fig. 1) and Shangri-La, north of Xanadu, near 2° N 150°. Dune faces illuminated by Cassini Radar in Belet were found to have slopes of ~10° and heights of ~100 m, values consistent with Cassini altimetry waveform simulations (Kirk et al., 2005; Callahan et al., 2006; Radebaugh et al., 2008). In radar, it is often possible to view interdune regions as separate from the dunes in radar signal and, therefore, material properties. The s°, or normalized backscatter coefficient, from dune materials on Titan and Earth are similar, enabling comparisons. Figures in this paper show that dune materials on Earth and Titan are generally dark to radar, and specifically Ku-band, with the exception of the slope illumination effects described above.

3. Analysis of processes

We use terrestrial radar and V-NIR images of dunes to inform us of processes and morphological interactions that occur in linear dune fields and apply those studies to Titan. This is done to better understand the conditions of sufficient wind speed to initiate and maintain saltation, sufficient sand supply, and depositional sinks that enable the formation and persistence of dunes on Titan.

3.1. Wind directions and interactions with topography

Before Cassini, it was known that Titan was favorable for aeolian transport, in that it has an atmosphere with a density at the surface 4 times higher than that of Earth, whereas the gravity is only one seventh that of Earth. Thus, relatively low winds suffice to move particulates (the optimum diameter particles of the order of 0.2 mm having a threshold windspeed of the order of 0.5–1 m/s). It was not clear pre-Cassini (Lorenz et al., 1995), however, whether enough sunlight was present to drive even these modest winds, nor whether vigorous sand-generating processes occurred. Furthermore, it was considered that liquid hydrocarbons on the surface might act as sand traps, and, thus, no strong reasons existed to expect dunes on Titan.

Dunes, however, are abundant on Titan (Lorenz et al., 2006; Radebaugh et al., 2008), covering most of the dark areas near the equator. The sand composition and formation process are not known, although a photochemical origin is suspected. The liquids on Titan are predominantly confined to high latitudes, and somehow (perhaps because of gravitational tides) near-surface winds are indeed large enough to effect transport (the Huygens probe measured winds of ~0.5 m/s close to the surface).

Dunes on Titan have dimensions and morphologies similar to those of linear dunes in the Namib and Saharan deserts (Lancaster, 1995; Lorenz et al., 2006; Radebaugh et al., 2008). Dunes of this type form on Earth in large sand seas, great sinks of sand located in the generally
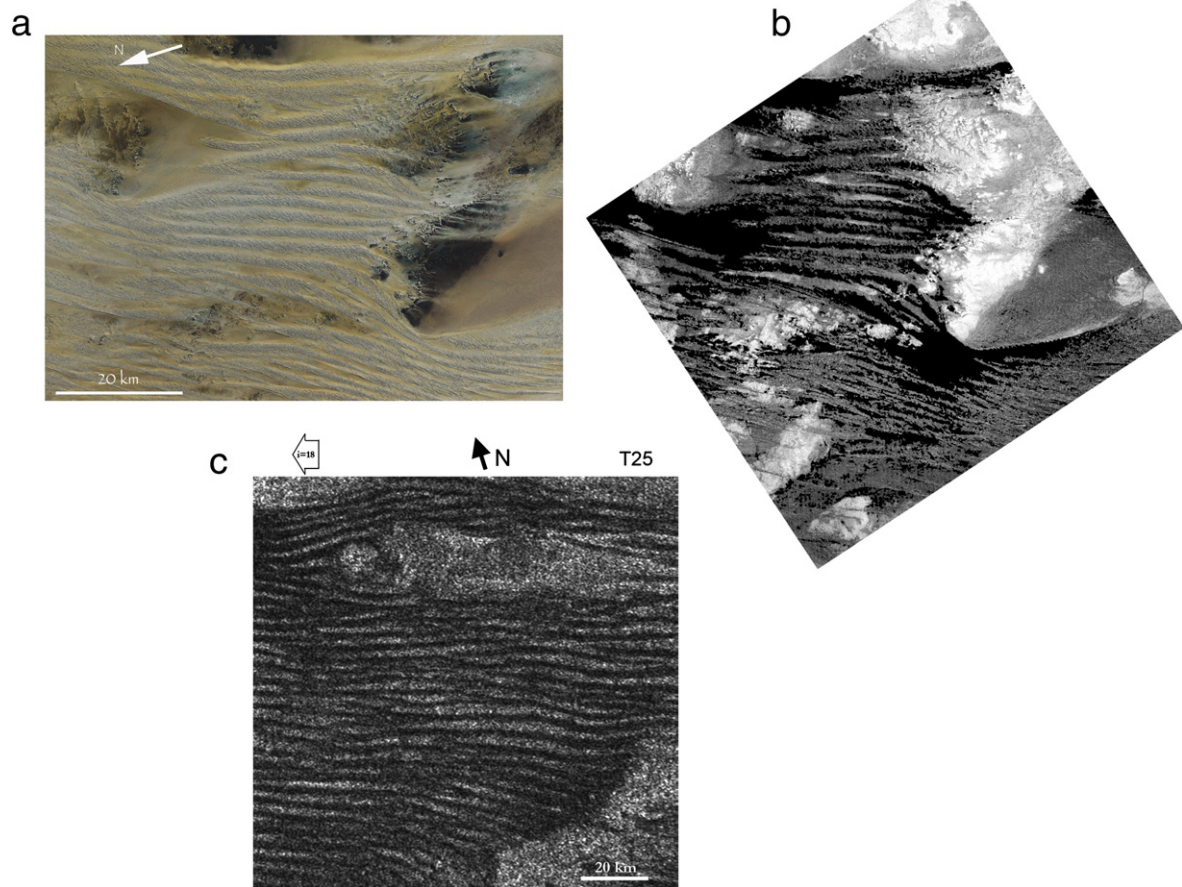

Fig. 4. a. Landsat image of linear dunes and topographic interactions in Libya, 22° 36″ N 20° 44″ E. Mean wind flow is L to R in the image, following the NE to SW trade winds. Dunes are light-colored while topographic obstacles are darker. b. SRTM C-band image of the same region; scale and north up are the same as in a. Landforms are radar-bright, while unorganized sands absorb the signal and appear dark. c. Dunes on Titan seen by Cassini Radar. These are in the Fensal sand sea, ~6° S, 40° W. Dune sands are radar-dark, while bright, elevated bedrock diverts the dunes. Note that with illumination along the dunes, no direct reflection from the slopes is possible, and they are uniformly dark. Image obtained during pass T25, Feb. 2007, 300 m resolution.

dry regions of western Namibia, western Egypt, Libya, Mauritania, and Saudi Arabia (Wilson, 1971; Kocurek et al., 1991; Lancaster, 1995). The dune forms were created mainly during the Pleistocene, when sand supply and winds were sufficient to draw out dunes into forms as great as 100 m high, 1–3 km wide, and hundreds of kilometers long. Currently active sand seas have highly efficient mechanisms of sand transport into, but not out of, sand sea regions, allowing for the maintenance of large features (Lancaster, 1995). Linear dune forms, also called "longitudinal" when dune formation and evolution processes and wind directions are being described, are typically created under conditions of seasonally alternating winds, likely from at least two widely separated directions (Tsoar, 1983; Rubin and Ikeda, 1990). The long axis of the dune forms along the resultant, time-averaged particle-transporting wind direction and sand transportation direction (Blandford, 1877; Fryberger and Dean, 1979). The authors have described the dunes on Titan as "longitudinal" in other papers; this paper uses "linear" to emphasize the dune form rather than the processes by which they were formed and evolve.

In sand sea regions where only dunes are visible, it can be difficult to determine which way winds of sufficient speeds blow to transport particles down the dune long axis. Dunes in sand seas, however, often interact with topographic obstacles, making the direction of high-velocity flow more clear. Fig. 4.a,b of Libya, for example, shows dunes diverging around topographic obstacles then resuming the original orientations on the downwind side, beyond a dune-free region similar to those observed in the Kalahari and elsewhere (Lancaster, 1988). Particle-transporting winds here appear to be flowing from L to R in the image (NE to SW). Dunes not able to completely skirt the elevated form sometimes stop abruptly, for example at the dark mountain in the lower right of the Landsat image, while high-resolution image details show sand streaks on the downwind side of the mountain, confirming recent NE to SW flow. Bedrock in the SRTM image (Fig. 4.b) has a large contrast to the dune regions; it appears very radar-bright because of rough terrain that scatters well at the C-band wavelength. Sands not organized into dunes appear radar-dark, especially at the N and S ends of the mountains, where winds have been diverted. Transverse dunes, sitting atop the linear dunes, are quite apparent in the Landsat image (Fig. 4.a), and even partially in the SRTM image (Fig. 4.b), indicating the most recent particle-moving wind flow was parallel to the dune axes.

Such details visible in the images of Libya (Fig. 4.a,b) cannot be seen in the lower-resolution Cassini Radar images of dunes on Titan (Fig. 4.c), but the dune interactions with topographic obstacles are similar. Dune sands, dark to radar because of the signal absorbing effects of the sand and the smooth dune surfaces, abut topographic obstacles, bright to radar because of rough, mainly water ice bedrock and radar-facing bedrock facets. On the western edge of the bright features, which are likely at least slightly elevated over the dune areas,
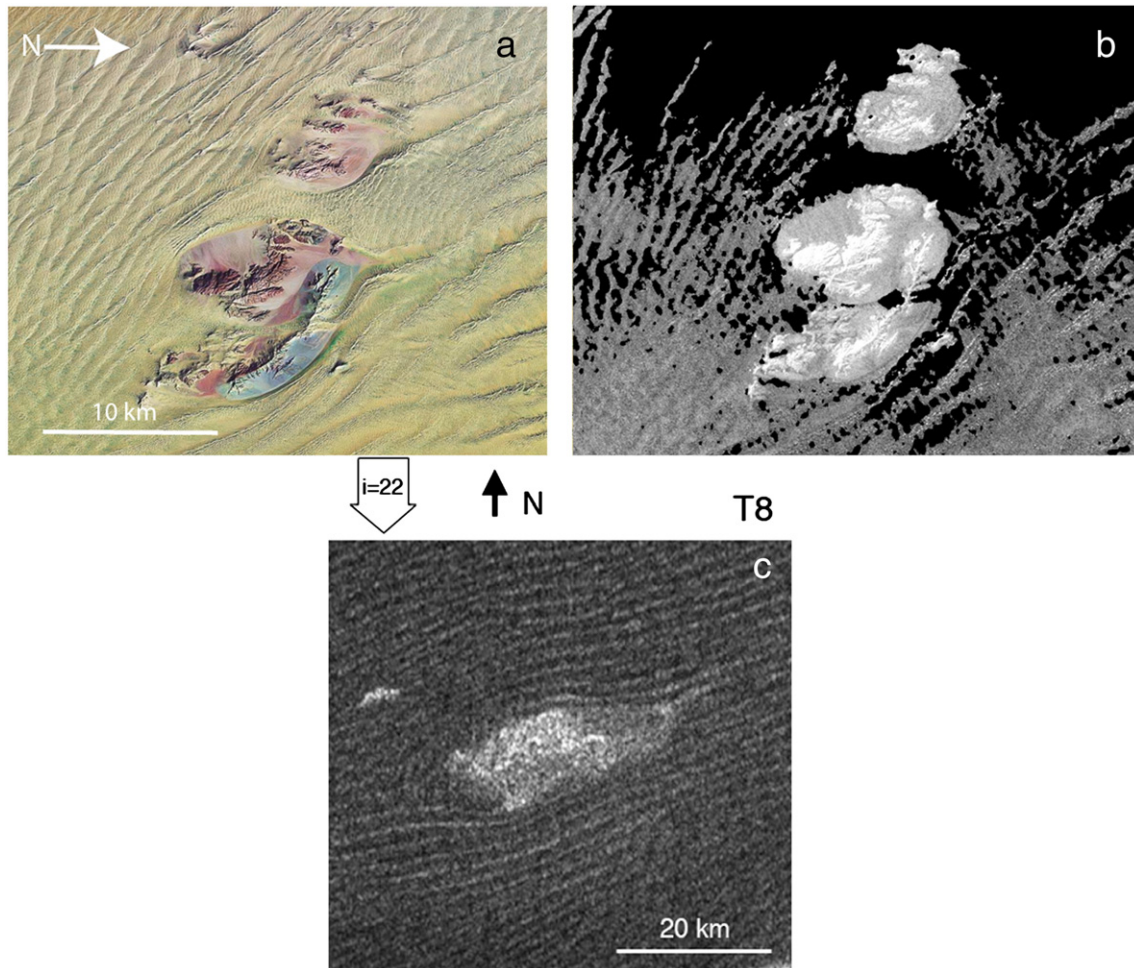

Fig. 5. a, b. Dune interactions with topographic obstacles in Namibia from Landsat 7 ETM+ and SRTM C-band. Substrate is only visible in mountainous regions, otherwise sand coverage is thick here. The radar image (b) shows bedrock as bright and unorganized dune sands as dark (black areas are unprocessed voids). Centered on 25° 23′ S 15° 16′ E, winds blow SE to NW. c. Similarly, dune sands are thick in this region of the Belet sand sea of Titan, where dunes divert around topographic obstacles and resume on the downwind side, similar to (a, b). Cassini Radar image centered on 6.5° S, 251° W, winds blow SW–NE (L–R). Image obtained during T8, Oct. 2005, 300 m resolution.

dunes are diverted to the north or south of the feature or stop abruptly where this diversion is not possible. Minor deviations from strictly linear in form can be seen in dunes at the south end of the image, perhaps because of diversion of winds from the typical, linear dune-forming patterns (Radebaugh et al., 2008). Dunes then resume the pattern on the downwind side of obstacles, similar to what is observed in Fig. 4.a,b. Based partly on such dune/topography observations, it has been inferred that mean, particle-moving wind flow on Titan is from the west to the east, with outlier deviations of up to 30° from east (Radebaugh et al., 2008). Such uniformity in wind direction across the globe has important implications for global-scale winds and atmospheric circulation patterns.

Tokano (2008) has attempted to reproduce the observed dune pattern on Titan with the winds in a Global Circulation Model (GCM), without success, suggesting some major unknowns about the angular momentum balance in the atmosphere. On the other hand, models (e.g. Mitchell, 2008) produce a humidity pattern that suggests that for reasonable assumptions about the methane moisture inventory on Titan, the tropics (<30° latitude) should dry out on relatively short timescales, consistent with the dryness required for mobilization of sand and lack of sand-trapping lakes in the latitude range over which dunes are observed.

A more close-up analysis of linear dune interactions with topography can be seen in Fig. 5. A Landsat 7 ETM+ image of dunes in Namibia (Fig. 5.a.) shows at least three separate scales of dunes: large, linear dunes oriented N–S, transverse dunes with NW–SE oriented axes, and smaller-scale, transverse dunes associated with winds blowing between the topographic obstacles. Wind streaks confirm the most recent particle-moving wind direction is to the N. Similar to Fig. 4.a., the linear dunes end abruptly upwind of the obstacles or divert around them, then resume on the downwind side. The other dune forms indicate winds are blocked and diverted near obstacles, especially at the upwind margins. Here, as well as between topographic obstacles, more uni-directional winds prevail, leading to small regions of transverse dunes. A SRTM C-band image of the same region (Fig. 5.b) shows exposed bedrock as bright, because of radar-facing slope reflections and roughness at the radar wavelength scales, and shows unorganized sands as dark. Note especially the smaller-scale, transverse dunes between mountains are radar dark, indicating sands are thick here. These small-scale patterns are not always visible in the lower-resolution Cassini Radar images, but a presence can be inferred from the terrestrial analogues, from the existence of regions that are more uniformly radar-dark, and from disruption in the normal linear dune pattern in the Cassini Radar images. Dune tops in the SRTM image (Fig. 5.b) are radar-bright, because of reflections off the seifs, or blade-like dune summits, as is also seen in the Landsat image (Fig. 5.a). Fig. 5.c is an image of dunes in the Belet sand sea interacting with an elevated obstacle. Dune faces are bright on the radar-facing slopes, indicating measurable slopes and heights of dune forms. The dunes show a clear streamlined form because of interaction with the obstacle on Titan (Fig. 5.c), similar to Fig. 5.a,b, resembling streamlined islands in a river. Upwind of the obstacle, the topographic obstacle margin is blunt, as in the Namib and Libya analogues, and the linear dunes appear to begin changing orientations upwind of the obstacles. This pattern is seen in other regions on Titan, and has also been observed on Earth (e.g., Bullard and Nash, 1998). A large-scale example of this on Titan is the upwind diversion of the dune field across several hundred kilometers extent west of the Xanadu region (Radebaugh et al., 2008).

3.2. Canyons, ridges, and craters

Often, terrestrial sand sea margins can be defined by topographic obstacles (Mainguet and Callot, 1978; Lancaster, 1995). The northern margin of the Namib sand sea ends abruptly at a canyon, and close-up images reveal the sands being transported northward directly into the canyon (Fig. 6), depriving the northern side of the canyon of dune-forming sands. This has also been studied in the Kalahari (Bullard and Nash, 1998). Some indication exists that similar processes happen on Titan, although because of the generally subdued topography on Titan (e.g. Radebaugh et al., 2007) and the resolution of the Cassini Radar, it can be difficult to determine in a few cases if topographic features are

Fig. 6. Dunes from the Namib Sand Sea migrate north to the Kuiseb River, where the sands are deposited into the river bed. Transport of dune materials to the west by fluvial action prevents dunes from continuing to form and migrate north of the river. Image credit GoogleEarth.

ridges, with raised topography, or river beds or canyons, with depressed topography, similar to the situation in Namibia.

When dunes interact with these morphological obstacles, sometimes they resume immediately downwind, indicating the river has cut through the sediments with no other associated alteration of the dune field (e.g., Lancaster, 1988; Bullard and Nash, 1998). On Titan, this morphology has only been verified in one case, when data existed from Cassini Radar and VIMS (Barnes et al., 2008). More often a dune-free region exists for several tens of kilometers past the feature, whereupon they partially resume the downwind course (e.g., Lancaster, 1988). Dunes in Yemen and on Titan (Fig. 7) approach roughly N–S trending linear features, at which the dunes end abruptly. In Yemen, this feature is a ridge, as can be seen in the Landsat (Fig. 7.a) and SRTM C-band (Fig. 7.b) images. The ridge is dark in Landsat and different from the surrounding tan dunes, and is bright in radar, indicating rough topography. Fig. 7.c shows dunes on Titan interacting with a Radar-dark obstacle, the nature of which is difficult to determine, given the Cassini Radar image resolution. If this feature is a river channel, then it may be a rare instance of a river channel that has more recently been active than the dunes in that region. This feature does not resemble, however, other channels on Titan, which are typically narrower and brighter, because of the presence of eroded bed materials. The feature, and the associated dune interactions, instead resembles the ridge in Yemen (Fig. 7.a,b) that precludes the

migration of dunes in the region. Several other features that indicate morphological controls on dune migration and dune field margins have been seen in Cassini Radar images.

Studies of wind flow over obstacles indicate wind flow is reduced on the downwind side, interrupting normal processes of dune formation (Pearse et al., 1981). Although wind conditions and sand supply may preclude the formation of dunes behind obstacles, sands may still be transported over these regions. In addition, sands may be carried laterally across linear dune fields by the alternating winds that lead to the dune forms. This explains why dunes eventually reappear some kilometers downwind of obstacles.

A structural feature of more planetary than terrestrial significance in terms of occurrence is the impact crater. Though Mars has extensive examples of dune interactions with impact craters, several instances of dune interactions with impact craters (or possible impact craters) also occur on Titan and on Earth. One such structure on Earth with dune interactions is Roter Kamm, found on the south end of the Namib Sand Sea (Fig. 8a,b). This feature is 2.5 km in diameter, and though fairly eroded, has a well-preserved rim. Dated at ~3.7 million years old, it is interesting to note the degree of invasion of the crater interior with dune sands. It is possible that up to 500 m thickness of sediment fills the crater interior (Fudali, 1973; Grant et al., 1997). Individual dunes can be distinguished within the crater in the Landsat image (Fig. 8.a) but they cannot in the SRTM C-band image (Fig. 8.b; Grant
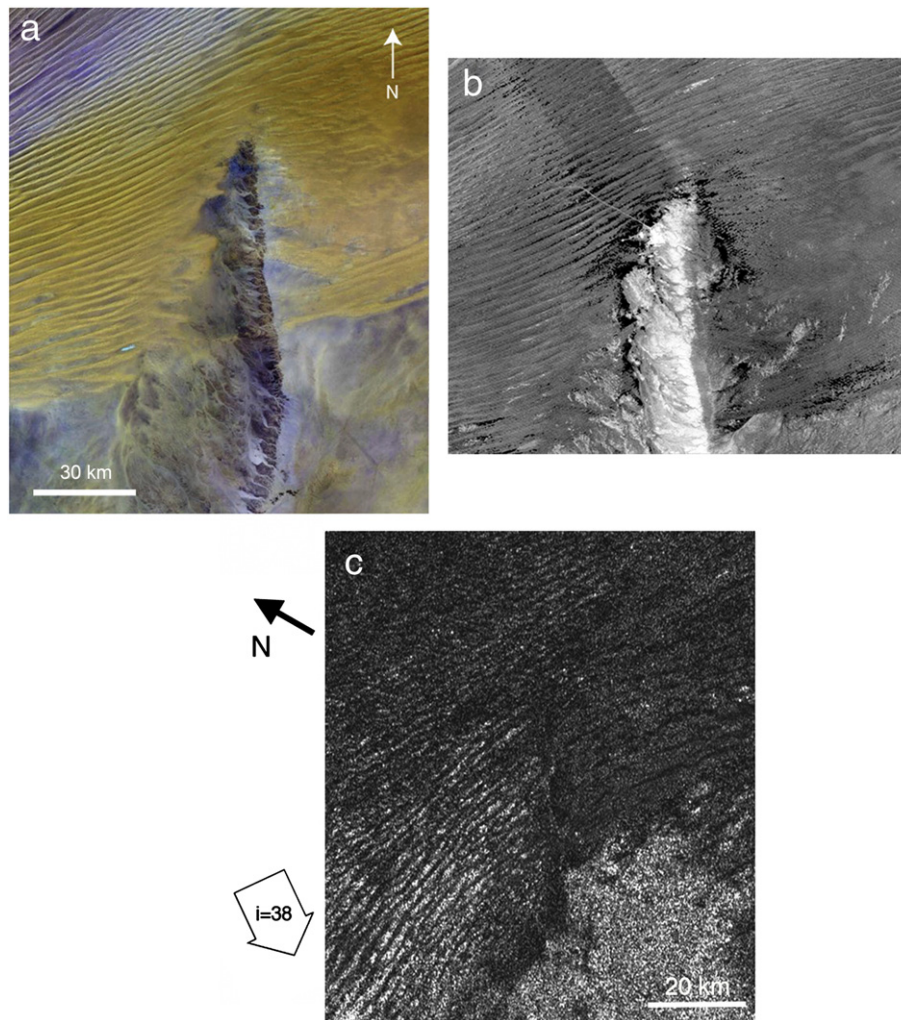

Fig. 7. Dunes interacting with topographic obstacles in Yemen (a, b) and Titan (c). a is a Landsat view of dunes in Yemen interacting with a dark, high ridge, centered at 17° 09″ N, 47° 10″ E. b is a SRTM C-band enlargement of the northern portion of the ridge. Sands not organized into dunes appear as radar-dark, whereas some dune summits appear bright dune to radar reflections. c is a Cassini Radar view of dunes on Titan interacting with a radar-dark feature. Dunes in Yemen and Titan abut the obstacle on the west, then are narrow and widely spaced for tens of kilometers beyond the obstacle. Titan image from the T17 flyby, Sep 2006, 6° N 37° W.
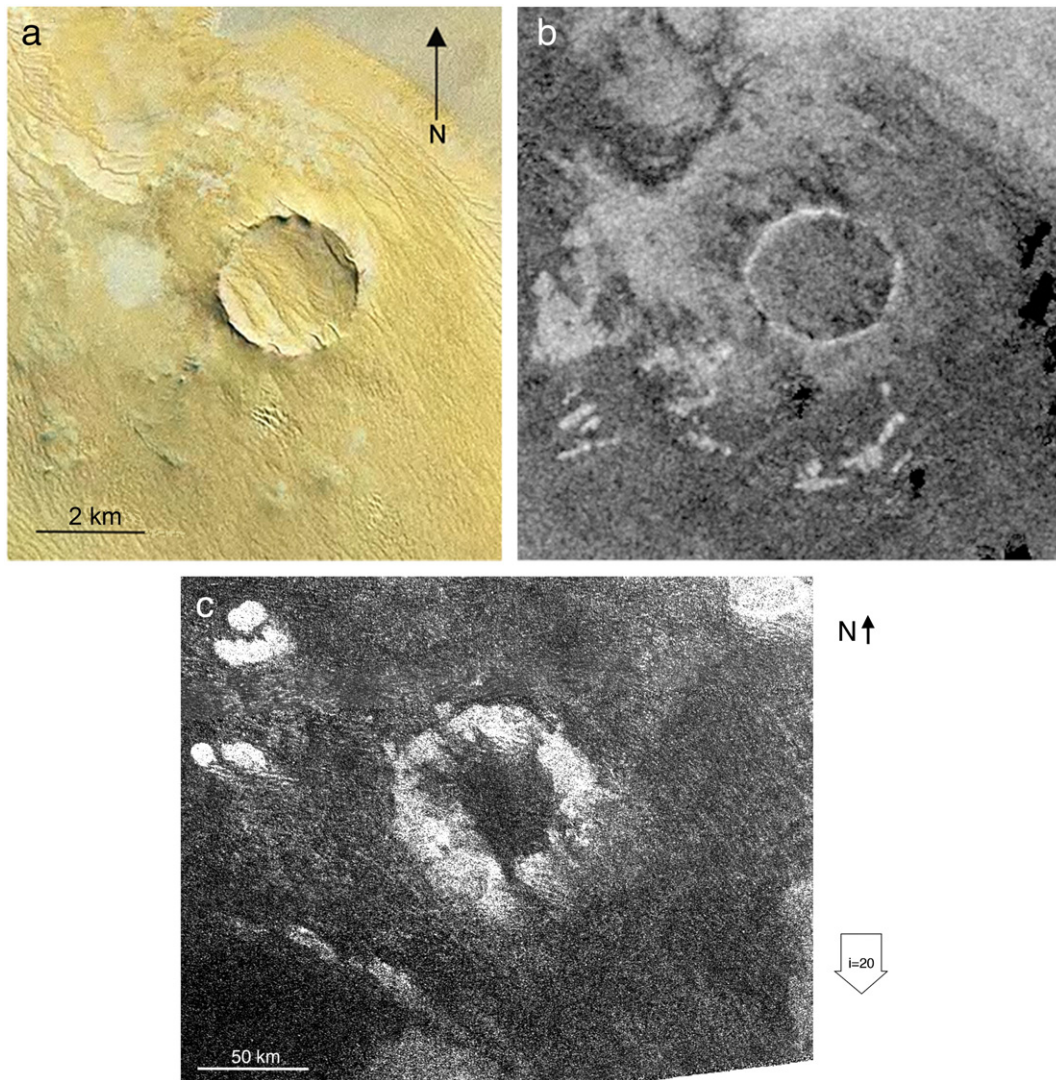
Fig. 8. a. Landsat image of dunes encroaching on Roter Kamm, an impact crater at the S end of the Namib Sand Sea. The circular crater is 2.5 km diameter, ~3.7 my old, and is located at 27° 5″ S, 16° 2″ E. North is up. b. SRTM C-band image of same region. Crater rim is visible as a bright ring, and substrate and surrounding mountains are also bright. Dunes range from grey to black, with no signal returned (void) for the thickest sand regions. c. Dunes encroach on Guabonito, a possible impact crater on Titan. Feature is ~90 km to outer edge and is located at 8° S 151° E. Image by Cassini Radar, T13 flyby, April 2006, 300 m resolution.

et al., 1997). The thick sands here are generally highly absorbing to radar, although as discussed in Blumberg (1998) low-incidence radar observations can show dunes as bright when the dune facets are presented normally to the radar illumination. Regions of especially thick dune sands return too little radar signal and appear black in the image. Other bedrock materials are visible to the radar through the overlying dune sands (Fig. 8.b). Other such structures where dunes and craters interact are found on Earth, such as the Arkenu structure (Paillou et al., 2003) and the Aorounga structure in Chad, which is overrun by linear dunes (Koeberl et al., 2005).

Fig. 8.c. shows a possible impact structure on Titan, called Guabonito. This feature is about 90 km in diameter (to the outer bright edge), has a round but highly eroded rim, and has been nearly fully encroached by dune sands, similar to Roter Kamm. Some individual dunes may be visible in this Cassini Radar image (Fig. 8.c). Clearly, it follows that with rates of sand transport on Earth, the rim can be breached and the floor of the crater filled on a timescale less than a few million years. Application of such reasoning to determine the age of Guabonito may not be particularly constraining in that the overall crater retention age of Titan seems to be of the order 500 million years (Lorenz et al., 2007). Rates of sand transport may be similar under Titan conditions to those on Earth (see Lorenz et al.,

2006), but Guabonito is an order of magnitude larger than Roter Kamm, suggesting perhaps that Guabonito is more than some tens of millions of years old. The rate of fill of Roter Kamm is only an upper limit, so no useful age constraint can really be inferred for Guabonito.

3.3. Dune transitions

Because of the sizes and locations in large deserts, linear dunes are the most areally extensive dune form on Earth (Lancaster, 1995). Yet the initiation and time evolution of this dune type is not well understood. One model for the formation of linear dunes from a preexisting dune form involves the elongation of one horn of a barchan dune into a linear dune (e.g., Bagnold, 1941). Because barchan dunes often form in regions of low sand supply, whereas linear dunes are stable in a wider range of sand supply, this transition may occur when sand supply has increased in a region. For example, a region occurs at the southern end of the Namib sand sea (Fig. 9.a,b,c) where sand supply is limited. Here, barchan dunes, typical dune forms in regions with sparse sand and uni-directional winds, show some of the horns being elongated into linear dunes (Fig. 9.b,c), perhaps because sand is being fed from surrounding regions or because the wind
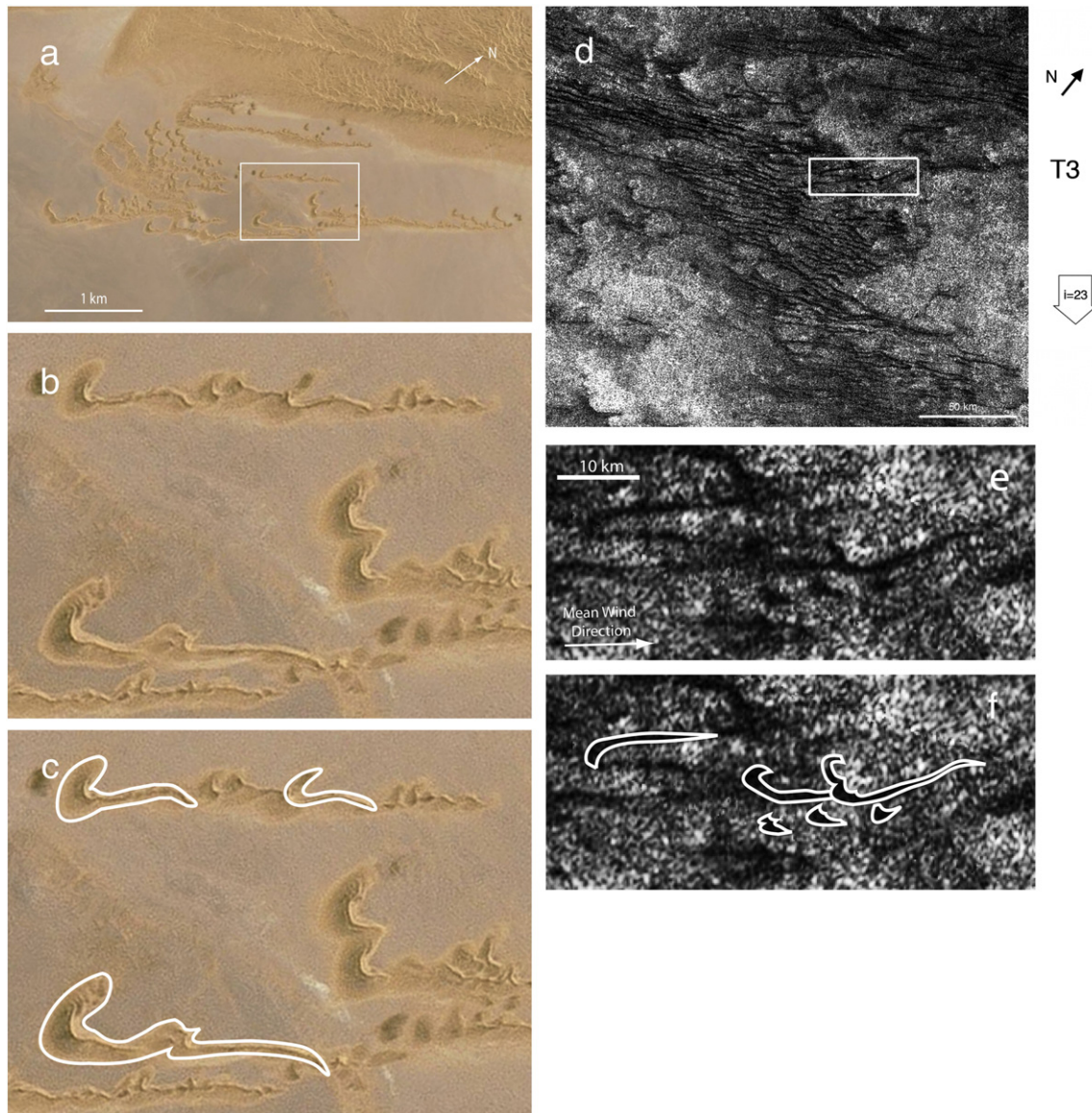
Fig. 9. Transition from barchan to linear dunes on Earth and Titan through elongation of barchan horns into linear dunes. a. Transitional dunes in Namibia (23° 48′22″ S, 15° 5′08″ E) show evidence of taking form similar to linear dunes to the NW. b is a close-up of white-boxed region in a, and c shows transitional forms outlined. d shows similar transitions in a dune field on Titan obtained during the T3 flyby, Feb. 2005 (12° N 105.3° W). e is an enlargement of the white-boxed region in d, and f shows transitional forms outlined. Note the scales are different between Earth and Titan, yet the forms are morphologically similar. Dune-transporting winds in the Earth and Titan images blow from left to right.

regime favors linear dune formation. A similar situation may exist in a higher-latitude region on Titan (Fig. 9.d,e,f), where sands may be of limited supply. Despite the lower image resolution of the Cassini Radar, it is possible to discern some forms that may be barchan dunes, one horn of each having elongated into a linear dune (Fig. 9.e,f). These relationships help establish the regional conditions of the dune areas; in regions on Earth and Titan in Fig. 9 the sand supply is limited, leading to transitional dune forms. Other transitional dune forms, such as barchan chains (e.g., Bourke, 2006), have also been observed on Titan, again at a resolution that makes it difficult to classify all aspects of the morphologies (Spencer et al., 2007).

4. Discussion/conclusions

These few but representative analogue studies illustrate the utility of comparative analyses of high-resolution terrestrial images of regions of known geology with new Cassini Radar images of Titan. The remarkable similarity of the dunes on Titan, albeit seen with relatively poor resolution (~300 m), to the linear dunes seen on Earth shows that terrestrial dunes, which are amenable to remote sensing by other techniques as well as field investigation, can be used as viable analogs to understand Titan.

Morphological studies can be done using V-NIR images such as Landsat ETM+, which present familiar colors and remote sensing resolutions to the scientist. Radar images are also powerful tools for morphological analyses, and in particular for revealing topography and shape. Often, the contrast in radar images between dunes and any interdune substrate is rather larger than is typical for optical images. We suggest that radar images are an underexploited resource for terrestrial dune studies.

Studies of these terrestrial analogues confirm that the primary conditions of 1 — sufficient winds, 2 — sand supply, and 3 — a depositional sink must be met for linear dunes to form and persist (Radebaugh et al., 2008). All analogue regions are in deserts of Earth, where sands can stay mobilized and not be carried away by rainfall or rivers, and where persistent winds blow or blew in the past to form the linear dunes. We assume such conditions exist on Titan as well, and that these studies will help further constrain the conditions for

dune formation. The 1.5 bar, mostly N_2 atmosphere of Titan appears to experience (now or in the past) global, particle-moving winds in a generally W–E direction at equatorial regions. Dunes on Titan give a unique constraint on these global circulation patterns (and the models do not yet agree with the data, perhaps indicating some as-yet-not-understood effect of large-scale topography; Lorenz and Radebaugh, 2009). Some superficial ambiguity occurs in inferring the direction of winds from linear dunes, but more careful inspection of the interaction of dunes with small-scale topographic obstacles allows this ambiguity to be resolved with some confidence; comparisons with terrestrial analogs are important in this exercise.

Whereas the interpretation of the radar images of dunes is reasonably straightforward, in that the sand (if dry) represents a homogenous dielectric target, interdunes reveal much more about sand volumes and properties of the substrate. Interdunes may be covered with a thin sheet of sand that renders them optically similar to the dunes (although in some locations they are optically different; Barnes et al., 2008), but may allow radar to penetrate some decimeters and reveal hidden textures. A better understanding of the depths of penetration of the Cassini Radar signal will help refine initial estimates of global dune sand volumes ($>2 \times 10^5$ km^3, Lorenz et al., 2008), providing valuable limits on atmospheric production of these materials. Analysis of radiometric and dielectric properties of terrestrial analogues will provide a wealth of information on material properties.

Beyond the purely geomorphological utility of radar imaging of dunes, it has application in the certification of landing sites for future space missions. In particular, a recent NASA Flagship mission study for combined orbiter-balloon-lander exploration of Titan (e.g. Leary et al., 2007; Lockwood et al., 2008) considered the Belet dunefield as a good target site. Whereas dunes entail possible steep slopes (and indeed slope failures) the aeolian sorting of material typically precludes rock hazards. Radar backscatter and radarclinometry methods can be used to apply limits to bright bedrock hazards and slopes amenable to lander safety.

Acknowledgments

References

Bagnold, R., 1941. Physics of wind-blown sand and desert dunes. W. Morrow and Co., New York. 265 pp.
Barnes, J.W., Brown, R.H., Soderblom, L., Sotin, C., Le Mouelic, S., Rodriguez, S., Jaumann, R., Beyer, R.A., Clark, R., Nicholson, P., 2008. Spectroscopy, morphometry, and photoclinometry of Titan's dunefields from Cassini/VIMS. Icarus 195, 400–414.
Blandford, W.T., 1877. Geological notes on the great desert between Sind and Rajputana. Geol. Surv. India Rec. 10, 10–21.
Blom, R., Elachi, C., 1981. Spaceborne and airborne imaging radar observations of sand dunes. J. Geophys. Res. 86, 3061–3073.
Blom, R., Elachi, C., 1987. Multifrequency and multipolarization radar scatterometry of sand dunes and comparison with spaceborne and airborne radar images. J. Geophys. Res. 92, 7877–7889.
Blumberg, D.G., 1998. Remote sensing of desert dune forms by polarimetric synthetic aperture radar (SAR). Remote Sens. Environ. 65, 204–216.
Blumberg, D.G., 2005. Analysis of large aeolian (wind-blown) bedforms using the Shuttle Radar Topography Mission (SRTM) digital elevation data. Remote Sens. Environ. 100, 179–189.
Bourke, M.C., 2006. A new model for linear dune formation: merged Barchan convoys on mars. Lunar Planet. Sci. XXXVI, 2432 (abstract).
Bullard, J.E., Nash, D.J., 1998. Linear dune pattern variability in the vicinity of dry valleys in the southwest Kalahari. Geomorphology 23, 35–54.
Callahan, P.S., Hensley, S., Gim, Y., Johnson, W.T., Lorenz, R.D., Alberti, G., Orosei, R., Seu, R., Franceschetti, G., Paillou, P., Paganelli, F., Wall, S., West, R.D., 2006. Information on Titan's surface from Cassini Radar Altimeter waveforms. Eos Trans. AGU 87 (52), P13A–0165 (Fall Suppl.).
Campbell, B.A., Campbell, D.B., 1992. Analysis of volcanic surface morphology on Venus from comparison of Arecibo, Magellan, and terrestrial airborne radar data. J. Geophys. Res. 97, 16293–16314.
Davis, P.A., Soderblom, L.A., 1984. Modeling crater topography and albedo from monoscopic Viking Orbiter images I-Methodology. J. Geophys. Res. 89, 9449–9457.
Elachi, C., Wall, S., Allison, M., Anderson, Y., Boehmer, R., Callahan, P., Encrenaz, P., Flameni, E., Franceschetti, G., Gim, Y., Hamilton, G., Hensley, S., Janssen, M., Johnson, W., Kelleher, K., Kirk, R., Lopes, R., Lorenz, R., Lunine, J., Muhleman, D., Ostro, S., Paganelli, F., Picardi, G., Posa, F., Roth, L., Seu, R., Shaffer, S., Soderblom, L., Stiles, B., Stofan, E., Vetrella, S., West, R., Wood, C., Wye, L., Zebker, H., 2005. Cassini radar views the surface of Titan. Science 308, 970–974.
Evans, D.L., Plaut, J.J., Stofan, E.R., 1997. Overview of the spaceborne imaging radar-C/X-synthetic. Remote Sens. Environ. 59, 135–140.
Farr, T.G., 2004. Terrestrial analogs to Mars: the NRC community decadal report. Planet. Space Sci. 52, 3–10.
Farr, T.G., Caro, E., Crippen, R., Duren, R., Hensley, S., Kobrick, M., Paller, M., Rodriguez, E., Rosen, P., Roth, L., Seal, D., Shaffer, S., Shimada, J., Umland, J., Werner, M., Oskin, M., Burbank, D., Alsdorf, D., 2007. The Shuttle radar topography mission. Rev. Geophys. 45. doi:10.1029/2005RG000183.
Fryberger, S.G., Dean, G., 1979. Dune forms and wind regime. In: McKee, E.D. (Ed.), A study of global sand seas. U.S. Geol. Surv. Prof. Pap., vol. 1052, pp. 137–169.
Fudali, R.F., 1973. Roter Kamm: evidence for an impact origin. Meteoritics 8, 245–257.
Grant, J.A., Koeberl, C., Reimold, W.U., Schultz, P.H., 1997. Gradation of the Roter Kamm impact crater, Namibia. J. Geophys. Res. 102, 16327–16338.
Greeley, R., Blumberg, D., McHone, J.F., Dobrovolskis, A., Iverson, J.D., Lancaster, N., Rasmussen, K., Wall, S.D., White, B.R., 1997. Applications of spaceborne radar laboratory data to the study of aeolian processes. J. Geophys Res 102, 10971–10983.
Greeley, R., Sullivan, R., Coon, M.D., Geissler, P.E., Tufts, B.R., Head, J.W., Pappalardo, R.T., Moore, J.M., 1998. Terrestrial sea ice morphology: considerations for Europa. Icarus 135, 25–40.
Keszthelyi, L., McEwen, A., 2007. Comparison of flood lavas on Earth and Mars. In: Chapman, M.G. (Ed.), The Geology of Mars: Evidence from Earth-Based Analogs. Cambridge University Press, Cambridge, UK, p. 126.
Kirk, R.L., Callahan, P., Seu, R., Lorenz, R.D., Paganelli, F., Lopes, R.M., Elachi, C., Cassini Radar Team, 2005. Radar reveals Titan topography. Lunar Planet. Sci. XXXVI, 2227 (abstract).
Kocurek, G., Havholm, K.G., Deynoux, M., Blakey, R.C., 1991. Amalgamated accumulations resulting from climatic and eustatic changes, Akchar Erg, Mauritania. Sedimentology 38, 751–772.
Koeberl, C., Reimold, W.U., Cooper, G., Cowan, D., Vincent, P.M., 2005. Aorounga and Gweni Fada impact structures, Chad: remote sensing, petrography, and geochemistry of target rocks. Meteorit. Planet. Sci. 40, 1455–1471.
Lancaster, N., 1988. Development of linear dunes in the southwestern Kalahari, southern Africa. J. Arid Env. 14, 233–244.
Lancaster, N., 1995. The Geomorphology of Desert Dunes. Routeledge, London. 290 pp.
Leary, J., Jones, C., Lorenz, R., Strain, R.D., Waite, J.H., 2007. Titan Explorer NASA Flagship Mission Study JHU Applied Physics Laboratory. August, (public release version http://www.lpi.usra.edu/opag/Titan_Explorer_Public_Report.pdf January 2009).
LeGall, A., Janssen, M.A., Lorenz, R.D., Wye, L., Callahan, P., Hayes, A., Zebker, H., Paganelli, F., Radebaugh, J., 2008. Titan's dunes and interdunes: new insights from Cassini Radar observations. Eos Trans. AGU 89 (53), P21A–1310 (Fall Suppl.).
Lockwood, M.K., Leary, J.C., Lorenz, R., Waite, H., Reh, K., Prince, J., Powell, R., 2008. Titan Explorer. AIAA-2008-7071, AIAA/AAS Astrodynamics Specialist Conference, Honolulu, Hawaii. August.
Lorenz, R.D., Mitton, J., 2008. Titan Unveiled. Princeton University Press, Princeton NY.
Lorenz, R.D., Radebaugh, J., 2009. Global pattern of Titan's dunes: radar survey from the Cassini prime mission. Geophys. Res. Lett. 36. doi:10.1029/2008GL036850.
Lorenz, R.D., Lunine, J.I., Grier, J.A., Fisher, M.A., 1995. Prediction of Aeolian features on planets: application to Titan Paleoclimatology. J. Geophys. Res. 88, 26377–26386.
Lorenz, R.D., Wall, S., Radebaugh, J., Boubin, G., Reffet, E., Janssen, M., Stofan, E., Lopes, R., Kirk, R., Elachi, C., Lunine, J., Paganelli, F., Soderblom, L., Wood, C., Wye, L., Zebker, H., Anderson, Y., Ostro, S., Allison, M., Boehmer, R., Callahan, P., Encrenaz, P., Ori, G.G., Francescetti, G., Gim, Y., Hamilton, G., Hensley, S., Johnson, W., Kelleher, K., Mitchell, K., Muhleman, D., Picardi, G., Posa, F., Roth, L., Seu, R., Shaffer, S., Stiles, B., Vetrella, S., Flamini, E., West, R., 2006. The sand seas of Titan: Cassini RADAR observations of Longitudinal Dunes. Science 312, 724–727.
Lorenz, R.D., Wood, C.A., Lunine, J.I., Wall, S.D., Lopes, R.M., Mitchell, K., Paganelli, F., Anderson, Y.Z., Wye, L., Tsai, C., Zebker, H., Stofan, E.R., Cassini RADAR Team, 2007. Titan's young surface: initial impact crater survey by Cassini RADAR and model comparison. Geophys. Res. Lett. 34, L07204. doi:10.1029/2006GL028971.
Lorenz, R.D., Mitchell, K.L., Kirk, R.L., Hayes, A.G., Zebker, H.A., Paillou, P., Radebaugh, J., Lunine, J.I., Janssen, M.A., Wall, S.D., Lopes, R.M., Stiles, B., Ostro, S., Mitri, G., Stofan, E.R., Cassini RADAR Team, 2008. Titan's inventory of organic surface materials. Geophys. Res. Lett. 35, L02206. doi:10.1029/2007GL032118.
Mainguet, M., Callot, Y., 1978. L'erg de Fachi-Bilma (Tchad-Niger). Mem. Doc. CNRS 18, 178.
Markham, B.L., Barker, J.L., Kaita, E., Seiferth, J., Morfitt, R., 2003. On-orbit performance of the Landsat-7 ETM+ radiometric calibrators. Int. J. Remote Sens. 24, 265–285.
McEwen, A.S., 1991. Photometric functions for photoclinometry and other applications. Icarus 92, 298–311.
Mitchell, J., 2008. The drying of Titan's dunes: Titan's methane hydrology and its impact on atmospheric circulation. J. Geophys. Res. 113. doi:10.1029/2007JE003017.
Paillou, P., Rosenqvist, A., Malézieux, J.-M., Reynard, B., Farr, T., Heggy, E., 2003. Discovery of a double impact crater in Libya: the astrobleme of Arkenu. C.R. Acad. Sci. Paris, Geosci. 335, 1059–1069.
Pearse, J.R., Lindley, D., Stevenson, D.C., 1981. Wind flow over ridges in simulated atmospheric boundary layers. Boundary-Layer Meteorolgy 21, 77–92.
Qong, M., 2000. Sand dune attributes estimated from SAR images. Remote Sensing of the Environment. 74, 217–228.
Radebaugh, J., Lorenz, R., Kirk, R., Lunine, J., Stofan, E., Lopes, R., Wall, S., Cassini Radar Team, 2007. Mountains on Titan observed by Cassini Radar. Icarus 192, 77–91. doi:10.1016/j.icarus.2007.06.020.
Radebaugh, J., Lorenz, R., Lunine, J., Wall, S., Boubin, G., Reffet, E., Kirk, R., Lopes, R., Stofan, E., Soderblom, L., Allison, M., Janssen, M., Paillou, P., Callahan, P., Cassini

Radar Team, 2008. Dunes on Titan observed by Cassini Radar. Icarus 194, 690–703. doi:10.1016/j.icarus.2007.10.015.

Rubin, D.M., Ikeda, H., 1990. Flume experiments on the alignment of transverse oblique and longitudinal dunes in directionally varying flows. Sedimentology 37, 673–684.

Soderblom, L., Anderson, J., Baines, K., Barnes, J., Barrett, J., Brown, R., Buratti, B., Clark, R., Cruikshank, D., Elachi, C., Janssen, M., Jaumann, R., Kirk, R., Karkoschka, E., Lemouelic, S., Lopes, R., Lorenz, R., Lunine, J., McCord, T., Nicholson, P., Radebaugh, J., Rizk, B., Sotin, C., Stofan, E., Sucharski, T., Tomasko, M., Wall, S., 2007. Correlations between Cassini VIMS spectra and RADAR SAR images: implications for Titan's surface composition and the character of the Huygens Probe landing site. Planet. Space Sci. 55, 2025–2036.

Spencer, C., Radebaugh, J., Lorenz, R., Wall, S., Lunine, J., Kirk, R., Lopes, R., Stofan, E.R., Cassini Radar Team, 2007. Terrestrial and Martian analogues to the sand seas on Titan. Geol. Soc. Amer. Abstr. Programs 39, 571 Abstract 209-23.

Stofan, E.R., Evans, D.L., Schmullius, C., Holt, B., Plaut, J.J., van Zyl, J., Wall, S.D., Way, J., 1995. Overview of results of Spaceborne Imaging Radar-C, X-Band Synthetic Aperture Radar (SIR-C/X-SAR). IEEE Trans. Geosci. Remote Sensing 33, 817–828.

Tokano, T., 2008. Dune-forming winds on Titan and the influence of topography. Icarus 194, 243–262.

Tomasko, M.G., Archinal, B., Becker, T., Bézard, B., Bushroe, M., Combes, M., Cook, D., Coustenis, A., de Bergh, C., Dafoe, L.E., Doose, L., Douté, S., Eibl, A., Engel, S., Gliem, F., Grieger, B., Holso, K., Howington-Kraus, E., Karkoschka, E., Keller, H.U., Kirk, R., Kramm, R., Küppers, M., Lanagan, P., Lellouch, E., Lemmon, M., Lunine, J., McFarlane, E., Moores, J., Prout, G.M., Rizk, B., Rosiek, M., Rueffer, P., Schröder, S.E., Schmitt, B., See, C., Smith, P., Soderblom, L., Thomas, N., West, R., 2005. Rain, winds and haze during the Huygens probe's descent to Titan's surface. Nature 438, 765–778. doi:10.1038/nature04126.

Tsoar, H., 1983. Dynamic processes acting on a longitudinal (seif) dune. Sedimentology 30, 567–578.

Wilson, I.G., 1971. Desert sandflow basins and a model for the development of ergs. Geogr. J. 137, 180–199.

Zimbelman, J.R., Williams, S.H., 2007. Eolian dunes and deposits in the western United States as analogs to wind-related features on Mars. In: Chapman, M.G. (Ed.), The Geology of Mars: Evidence from Earth-Based Analogs. Cambridge University Press, Cambridge, UK, p. 126.